

# Proposal for a new scheme for producing a two-photon, high dimensional hyperentangled state

Hong-Bo Xu<sup>a</sup>, Kun Du<sup>a</sup> and Cong-Feng Qiao<sup>a,b\*</sup>

<sup>a</sup>Department of Physics, Graduate University of Chinese Academy of Sciences,  
Beijing 100049, China

<sup>b</sup>Theoretical Physics Center for Science Facilities (TPCSF),  
CAS, Beijing 100049, China

We propose an experimentally feasible scheme for generating a two  $2 \times 4 \times 4$  dimensional photons hyperentangled state, entangled in polarization, frequency and spatial mode. This scheme is mainly based on a parametric down-conversion source and cross-Kerr nonlinearities, which avoids the complicated uncertain post-selection. Our method can be easily expanded to the production of hyperentangled states with more photons in multidimensions. Hence the expectation for vast quantities of information in quantum information processing will possibly come true. Finally, we put forward a realizable quantum key distribution (QKD) protocol based on the high dimensional hyperentangled state.

**Keywords:** hyperentanglement; multidimension; quantum key distribution; Qudit

## 1 Introduction

Entanglement is viewed as a kind of raw resource of quantum information science, such as measurement-based quantum computing [1], quantum teleportation [2], quantum dense coding [3], entanglement purification [4] and quantum cryptography [5]. Thus far there have been plentiful protocols in quantum information processing by applying two-dimensional

---

\*Corresponding author. Email: qiaocf@gucas.ac.cn

quantum systems-qubits. Due to the demand for more and more information content, some research has focused on extending qubits to multidimensional entangled states-qudits. In recent years, three-dimensional quantum states (qutrits) [6, 7] and higher dimensional quantum states [8, 9, 10] have been experimentally realized. The qudits have shown better characteristics and advantages than qubits. For instance, multidimensional entanglement has shown stronger quantum nonlocality [11] and noise immunity [12]. Moreover, qudits can observably improve the security of quantum key distribution [13, 14, 15, 16].

Notwithstanding at present the relevant methods to prepare a state in arbitrary  $d$ -dimensional Hilbert space entangled in one degree of freedom (DOF) have been proposed, the experimental realization of multipartite entanglement is still a significant challenge. Being analogous to the case of qubits, hyperentanglement [17] provides an effective and practical capacity-increased way to manipulate more qudits in arbitrary desirable Hilbert dimensions. Furthermore, hyperentanglement is much less affected by decoherence and plays an important role in the realization of even more challenging quantum information processing in comparison with the normal entangled states.

In this paper, we propose a scheme for generating a two  $2 \times 4 \times 4$  dimensional photon hyperentangled state, entangled in polarization, frequency and spatial mode DOFs respectively. After that we discuss a feasible quantum key distribution protocol based on this hyperentangled state. Our protocol can observably increase the efficiency of key distribution and the flux of information.

## **2 Preparation scheme for multidimensional hyperentangled state**

In this section, a preparation scheme of the two  $2 \times 4 \times 4$  dimensional photon hyperentangled state, entangled in polarization, frequency and spatial mode, is introduced. By means of the scheme, the two photons are simultaneously entangled in polarization, frequency and spatial modes, encoded in two-dimensional, four-dimensional and four-dimensional Hilbert spaces respectively. The hyperentangled state takes the following form up to a normalization

constant:

$$|\psi\rangle = (HV + VH)(\omega_{11}\omega_{12} + \omega_{12}\omega_{11} + \omega_{21}\omega_{22} + \omega_{22}\omega_{21})(a_{11}b_{11} + a_{12}b_{12} + a_{21}b_{21} + a_{22}b_{22}), \quad (1)$$

where  $H$  and  $V$  denote horizontal and vertical polarization,  $\omega_{11}, \omega_{12}, \omega_{21}, \omega_{22}$  signify different frequencies and  $a_{11}, a_{12}, a_{21}, a_{22}$  and  $b_{11}, b_{12}, b_{21}, b_{22}$  label different spatial modes.

The first step is to produce primary light source which has the form as  $|\omega_1\rangle + |\omega_2\rangle$  ( $\omega_2 = 4\omega_1$ ) in frequency. The spatial mode of the Initial laser pulse is turned into a superposition of two new spatial modes by a 50:50 beam splitter (BS). Put two frequency multipliers (FM) [18] on the above path, and then the two paths are coupled with another BS. Right now the superposition of the two spatial modes has turned into a superposition of two new frequencies.

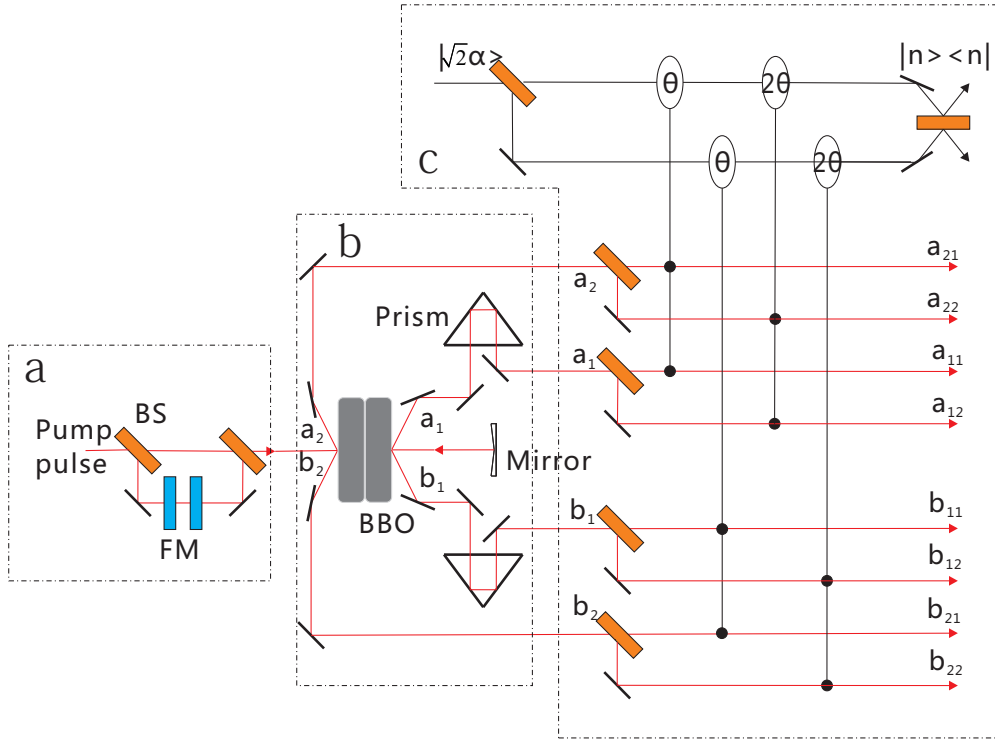


Figure 1: Preparation scheme of the two  $2 \times 4 \times 4$  dimensional photons hyperentangled state via type-II barium borate (BBO) crystal and cross-Kerr nonlinearity.

Then as shown in Figure 1 through two adjacent type-II barium borate (BBO) crystals [19], for the first (second) crystal, the ratio of the frequency of the signal photon to the frequency of the idler photon is 1:2 (2:1) [17], thus the photon pairs can be encoded in

two-dimensional polarization entanglement and four-dimensional frequency entanglement ( $|\omega_1\rangle=|\omega_{11}\rangle+|\omega_{12}\rangle$ ,  $|\omega_2\rangle=|\omega_{21}\rangle+|\omega_{22}\rangle$ ,  $\omega_{11}:\omega_{12}:\omega_{21}:\omega_{22}=1:2:4:8$ ) by spontaneous parametric down-conversion (SPDC) [20] and emitted into the spatial modes  $a_1$  and  $b_1$ . In case the pump pulse passes through the crystal with no photon pairs emitted, it will be reflected by the mirror and transit the crystal a second time, which may produce corresponding photon pairs in spatial modes  $a_2$  and  $b_2$  [21]. As a result, we encode the two-photon state in two-dimensional spatial mode entanglement as well. After eliminating the undesired timing information [22], the two-photon hyperentangled states in the following form are readily obtained:

$$|\psi\rangle = (HV + VH)(\omega_{11}\omega_{12} + \omega_{12}\omega_{11} + \omega_{21}\omega_{22} + \omega_{22}\omega_{21})(a_1b_1 + a_2b_2). \quad (2)$$

Next, let photons in every path enter a BS, so that every spatial mode is divided into two new spatial modes with equal probability and fixed phase relation. Since one can simply adjust the relative phase, the two-photon state in the new eight spatial modes can be expressed as  $(a_{11} + a_{12})(b_{11} + b_{12}) + (a_{21} + a_{22})(b_{21} + b_{22})$ .

Afterwards, these eight paths are led to a cross-kerr nonlinear medium [23, 24], which brings forth an adjustable phase shift to the coherent state through cross-phase modulation (XPM). First using a BS to divide the coherent state into two beams  $|\alpha\rangle$   $|\alpha\rangle$ , adjust the phase shifts of the upper  $|\alpha\rangle$  into  $\theta$ ,  $\theta$ ,  $2\theta$  and  $2\theta$  for modes  $a_{11}$ ,  $a_{21}$ ,  $a_{12}$  and  $a_{22}$  respectively. Analogously, modes  $b_{11}$ ,  $b_{21}$ ,  $b_{12}$  and  $b_{22}$  induce the phase shifts of the under  $|\alpha\rangle$  into  $\theta$ ,  $\theta$ ,  $2\theta$  and  $2\theta$  respectively. Then the two coherent states are compared with a BS. After projecting the  $|n\rangle\langle n|$  onto the upper beam [25, 26], if  $n = 0$ , the state in spatial mode transforms into  $a_{11}b_{11} + a_{12}b_{12} + a_{21}b_{21} + a_{22}b_{22}$ , i.e. four-dimensional spatial mode entanglement. Finally, the state (2) has turned into the state (1), the two  $2 \times 4 \times 4$  dimensional photons hyperentangled state is created.

A setup for measuring the hyperentanglement in polarization, frequency and spatial mode simultaneously and independently is schematically shown in Figure 2. Place eight of these setups in all eight output modes, then the qudits in spatial mode can be determined. Then every mode is split into four paths according to frequency by an optical demultiplexer (OD) [27], hence the qudits in frequency are obtained. Thereafter the conventional polarization

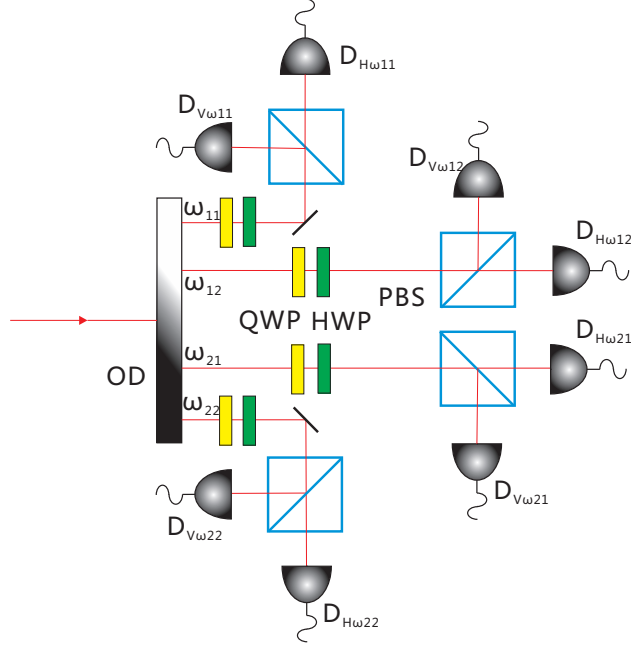


Figure 2: The setup for measuring the high dimensional hyperentangled state.

analysis [28] is applied in all the four paths in order to read out the qubits in polarization.

As the theory goes, our scheme can be simply expanded to the production of a hyperentangled state with an arbitrary number of photons and arbitrary dimensional entanglement, which will immensely increase the quantity of information.

### 3 QKD protocol for multidimensional hyperentangled state

Now we shall present a QKD protocol using the high dimensional hyperentangled state generated above. In our method, we utilize the four-dimensional hyperentanglement swapping [29] in frequency and spatial mode DOFs of the two photons lying in the state of following form:

$$\begin{aligned}
 |\psi\rangle = & (|\omega_{11}\rangle|\omega_{12}\rangle + |\omega_{12}\rangle|\omega_{11}\rangle + |\omega_{21}\rangle|\omega_{22}\rangle + |\omega_{22}\rangle|\omega_{21}\rangle) \\
 & (|a_{11}\rangle|b_{11}\rangle + |a_{12}\rangle|b_{12}\rangle + |a_{21}\rangle|b_{21}\rangle + |a_{22}\rangle|b_{22}\rangle).
 \end{aligned}
 \tag{3}$$

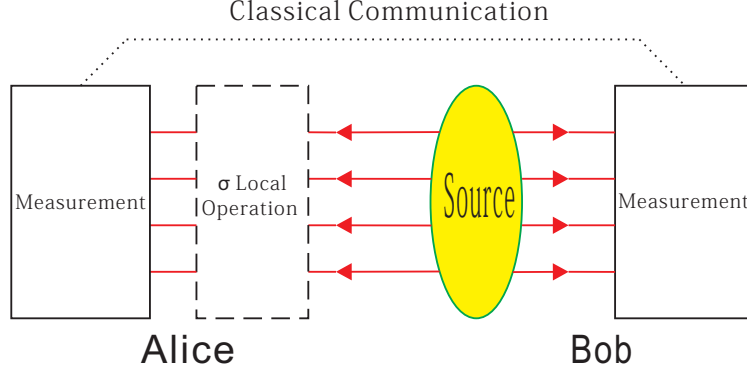


Figure 3: Scheme showing the principle of QKD protocol using high dimensional hyperentangled state.

As shown in Figure 3, send the two photons to Alice and Bob respectively, named photon A and photon B. Then the state (3) can be expressed as:

$$\begin{aligned}
|\psi\rangle = & \frac{1}{8}(|\psi_{11}\rangle_A|\psi_{11}\rangle_B + |\psi_{12}\rangle_A|\psi_{12}\rangle_B + |\psi_{13}\rangle_A|\psi_{13}\rangle_B + |\psi_{14}\rangle_A|\psi_{14}\rangle_B \\
& + |\psi_{21}\rangle_A|\psi_{21}\rangle_B + |\psi_{22}\rangle_A|\psi_{22}\rangle_B + |\psi_{23}\rangle_A|\psi_{23}\rangle_B + |\psi_{24}\rangle_A|\psi_{24}\rangle_B \\
& + |\psi_{31}\rangle_A|\psi_{31}\rangle_B + |\psi_{32}\rangle_A|\psi_{32}\rangle_B + |\psi_{33}\rangle_A|\psi_{33}\rangle_B + |\psi_{34}\rangle_A|\psi_{34}\rangle_B \\
& + |\psi_{41}\rangle_A|\psi_{41}\rangle_B + |\psi_{42}\rangle_A|\psi_{42}\rangle_B + |\psi_{43}\rangle_A|\psi_{43}\rangle_B + |\psi_{44}\rangle_A|\psi_{44}\rangle_B), \tag{4}
\end{aligned}$$

where

$$\begin{aligned}
|\psi_{11}\rangle_A &= \frac{1}{2}(|\omega_{11}\rangle|a_{11}\rangle + |\omega_{12}\rangle|a_{12}\rangle + |\omega_{21}\rangle|a_{21}\rangle + |\omega_{22}\rangle|a_{22}\rangle); \\
|\psi_{12}\rangle_A &= \frac{1}{2}(|\omega_{11}\rangle|a_{11}\rangle - |\omega_{12}\rangle|a_{12}\rangle - |\omega_{21}\rangle|a_{21}\rangle + |\omega_{22}\rangle|a_{22}\rangle); \\
|\psi_{13}\rangle_A &= \frac{1}{2}(|\omega_{11}\rangle|a_{11}\rangle - |\omega_{12}\rangle|a_{12}\rangle + |\omega_{21}\rangle|a_{21}\rangle - |\omega_{22}\rangle|a_{22}\rangle); \\
|\psi_{14}\rangle_A &= \frac{1}{2}(|\omega_{11}\rangle|a_{11}\rangle + |\omega_{12}\rangle|a_{12}\rangle - |\omega_{21}\rangle|a_{21}\rangle - |\omega_{22}\rangle|a_{22}\rangle); \\
|\psi_{21}\rangle_A &= \frac{1}{2}(|\omega_{11}\rangle|a_{12}\rangle + |\omega_{12}\rangle|a_{21}\rangle + |\omega_{21}\rangle|a_{22}\rangle + |\omega_{22}\rangle|a_{11}\rangle); \\
|\psi_{22}\rangle_A &= \frac{1}{2}(|\omega_{11}\rangle|a_{12}\rangle - |\omega_{12}\rangle|a_{21}\rangle - |\omega_{21}\rangle|a_{22}\rangle + |\omega_{22}\rangle|a_{11}\rangle); \\
|\psi_{23}\rangle_A &= \frac{1}{2}(|\omega_{11}\rangle|a_{12}\rangle - |\omega_{12}\rangle|a_{21}\rangle + |\omega_{21}\rangle|a_{22}\rangle - |\omega_{22}\rangle|a_{11}\rangle); \\
|\psi_{24}\rangle_A &= \frac{1}{2}(|\omega_{11}\rangle|a_{12}\rangle + |\omega_{12}\rangle|a_{21}\rangle - |\omega_{21}\rangle|a_{22}\rangle - |\omega_{22}\rangle|a_{11}\rangle);
\end{aligned}$$



$$\begin{aligned}
|\psi_{33}\rangle_B &= \frac{1}{2}(|\omega_{12}\rangle|a_{21}\rangle - |\omega_{11}\rangle|a_{22}\rangle + |\omega_{22}\rangle|a_{11}\rangle - |\omega_{21}\rangle|a_{12}\rangle); \\
|\psi_{34}\rangle_B &= \frac{1}{2}(|\omega_{12}\rangle|a_{21}\rangle + |\omega_{11}\rangle|a_{22}\rangle - |\omega_{22}\rangle|a_{11}\rangle - |\omega_{21}\rangle|a_{12}\rangle); \\
|\psi_{41}\rangle_B &= \frac{1}{2}(|\omega_{12}\rangle|a_{22}\rangle + |\omega_{11}\rangle|a_{11}\rangle + |\omega_{22}\rangle|a_{12}\rangle + |\omega_{21}\rangle|a_{21}\rangle); \\
|\psi_{42}\rangle_B &= \frac{1}{2}(|\omega_{12}\rangle|a_{22}\rangle - |\omega_{11}\rangle|a_{11}\rangle - |\omega_{22}\rangle|a_{12}\rangle + |\omega_{21}\rangle|a_{21}\rangle); \\
|\psi_{43}\rangle_B &= \frac{1}{2}(|\omega_{12}\rangle|a_{22}\rangle - |\omega_{11}\rangle|a_{11}\rangle + |\omega_{22}\rangle|a_{12}\rangle - |\omega_{21}\rangle|a_{21}\rangle); \\
|\psi_{44}\rangle_B &= \frac{1}{2}(|\omega_{12}\rangle|a_{22}\rangle + |\omega_{11}\rangle|a_{11}\rangle - |\omega_{22}\rangle|a_{12}\rangle - |\omega_{21}\rangle|a_{21}\rangle). \tag{5}
\end{aligned}$$

Consequently, in this way the hyperentanglement in frequency and spatial mode of the two photons has been expressed as the sum of 16 tensor products of each single photon's frequency-spatial mode entangled state. At the site of Alice, Alice can carry out  $\sigma$  local operation on the spatial mode of photon A. There are 16 local operations, and each corresponds to an encoding, i.e.

$$\begin{aligned}
\sigma_1 &\leftrightarrow (0000); \sigma_2 \leftrightarrow (0001); \sigma_3 \leftrightarrow (0010); \sigma_4 \leftrightarrow (0011); \\
\sigma_5 &\leftrightarrow (0100); \sigma_6 \leftrightarrow (0101); \sigma_7 \leftrightarrow (0110); \sigma_8 \leftrightarrow (0111); \\
\sigma_9 &\leftrightarrow (1000); \sigma_{10} \leftrightarrow (1001); \sigma_{11} \leftrightarrow (1010); \sigma_{12} \leftrightarrow (1011); \\
\sigma_{13} &\leftrightarrow (1100); \sigma_{14} \leftrightarrow (1101); \sigma_{15} \leftrightarrow (1110); \sigma_{16} \leftrightarrow (1111). \tag{6}
\end{aligned}$$

The results of these 16 local operations implemented on spatial mode  $|\psi\rangle_S = (|a_{11}\rangle|b_{11}\rangle + |a_{12}\rangle|b_{12}\rangle + |a_{21}\rangle|b_{21}\rangle + |a_{22}\rangle|b_{22}\rangle)$  are

$$\begin{aligned}
\sigma_1|\psi\rangle_S &\rightarrow |\psi_1\rangle_S = (|a_{11}\rangle|b_{11}\rangle + |a_{12}\rangle|b_{12}\rangle + |a_{21}\rangle|b_{21}\rangle + |a_{22}\rangle|b_{22}\rangle); \\
\sigma_2|\psi\rangle_S &\rightarrow |\psi_2\rangle_S = (|a_{11}\rangle|b_{11}\rangle - |a_{12}\rangle|b_{12}\rangle - |a_{21}\rangle|b_{21}\rangle + |a_{22}\rangle|b_{22}\rangle); \\
\sigma_3|\psi\rangle_S &\rightarrow |\psi_3\rangle_S = (|a_{11}\rangle|b_{11}\rangle - |a_{12}\rangle|b_{12}\rangle + |a_{21}\rangle|b_{21}\rangle - |a_{22}\rangle|b_{22}\rangle); \\
\sigma_4|\psi\rangle_S &\rightarrow |\psi_4\rangle_S = (|a_{11}\rangle|b_{11}\rangle + |a_{12}\rangle|b_{12}\rangle - |a_{21}\rangle|b_{21}\rangle - |a_{22}\rangle|b_{22}\rangle); \\
\sigma_5|\psi\rangle_S &\rightarrow |\psi_5\rangle_S = (|a_{11}\rangle|b_{12}\rangle + |a_{12}\rangle|b_{21}\rangle + |a_{21}\rangle|b_{22}\rangle + |a_{22}\rangle|b_{11}\rangle); \\
\sigma_6|\psi\rangle_S &\rightarrow |\psi_6\rangle_S = (|a_{11}\rangle|b_{12}\rangle - |a_{12}\rangle|b_{21}\rangle - |a_{21}\rangle|b_{22}\rangle + |a_{22}\rangle|b_{11}\rangle);
\end{aligned}$$

$$\begin{aligned}
\sigma_7|\psi\rangle_S &\rightarrow |\psi_7\rangle_S = (|a_{11}\rangle|b_{12}\rangle - |a_{12}\rangle|b_{21}\rangle + |a_{21}\rangle|b_{22}\rangle - |a_{22}\rangle|b_{11}\rangle); \\
\sigma_8|\psi\rangle_S &\rightarrow |\psi_8\rangle_S = (|a_{11}\rangle|b_{12}\rangle + |a_{12}\rangle|b_{21}\rangle - |a_{21}\rangle|b_{22}\rangle - |a_{22}\rangle|b_{11}\rangle); \\
\sigma_9|\psi\rangle_S &\rightarrow |\psi_9\rangle_S = (|a_{11}\rangle|b_{21}\rangle + |a_{12}\rangle|b_{22}\rangle + |a_{21}\rangle|b_{11}\rangle + |a_{22}\rangle|b_{12}\rangle); \\
\sigma_{10}|\psi\rangle_S &\rightarrow |\psi_{10}\rangle_S = (|a_{11}\rangle|b_{21}\rangle - |a_{12}\rangle|b_{22}\rangle - |a_{21}\rangle|b_{11}\rangle + |a_{22}\rangle|b_{12}\rangle); \\
\sigma_{11}|\psi\rangle_S &\rightarrow |\psi_{11}\rangle_S = (|a_{11}\rangle|b_{21}\rangle - |a_{12}\rangle|b_{22}\rangle + |a_{21}\rangle|b_{11}\rangle - |a_{22}\rangle|b_{12}\rangle); \\
\sigma_{12}|\psi\rangle_S &\rightarrow |\psi_{12}\rangle_S = (|a_{11}\rangle|b_{21}\rangle + |a_{12}\rangle|b_{22}\rangle - |a_{21}\rangle|b_{11}\rangle - |a_{22}\rangle|b_{12}\rangle); \\
\sigma_{13}|\psi\rangle_S &\rightarrow |\psi_{13}\rangle_S = (|a_{11}\rangle|b_{22}\rangle + |a_{12}\rangle|b_{11}\rangle + |a_{21}\rangle|b_{12}\rangle + |a_{22}\rangle|b_{21}\rangle); \\
\sigma_{14}|\psi\rangle_S &\rightarrow |\psi_{14}\rangle_S = (|a_{11}\rangle|b_{22}\rangle - |a_{12}\rangle|b_{11}\rangle - |a_{21}\rangle|b_{12}\rangle + |a_{22}\rangle|b_{21}\rangle); \\
\sigma_{15}|\psi\rangle_S &\rightarrow |\psi_{15}\rangle_S = (|a_{11}\rangle|b_{22}\rangle - |a_{12}\rangle|b_{11}\rangle + |a_{21}\rangle|b_{12}\rangle - |a_{22}\rangle|b_{21}\rangle); \\
\sigma_{16}|\psi\rangle_S &\rightarrow |\psi_{16}\rangle_S = (|a_{11}\rangle|b_{22}\rangle + |a_{12}\rangle|b_{11}\rangle - |a_{21}\rangle|b_{12}\rangle - |a_{22}\rangle|b_{21}\rangle). \tag{7}
\end{aligned}$$

Thus corresponding to the 16 local operations, the initial state  $|\psi\rangle$  will be turned into 16 kinds of form, for instance, the state (3) corresponds to operation  $\sigma_1$ .

After local operation, Alice measures the frequency-spatial mode entangled state of her photon by virtue of the measurement setup shown in appendix. Take the state (4) for example, in case the result obtained by Alice is  $|\psi_{11}\rangle_A$ , she tells Bob her result via classical communication. Depending on Alice's measurement result, Bob's photon will be projected to the corresponding state  $|\psi_{11}\rangle_B$ . Bob subsequently measures his photon with the same setup, his result will be  $|\psi_{11}\rangle_B$  which is perfectly correlated to Alice's result. Thereupon, according to Alice's result and his result, Bob can be well aware that the state after local operation must be the state (4), and the corresponding local operation is  $\sigma_1$ . In this way, Alice and Bob can take the encoding of  $\sigma_1$  as their determinate secure key, and the  $|\psi_{11}\rangle_B$  as random secure key.

In theory, this protocol can absolutely generate a four-bit determinate secure key and a four-bit random secure key for one pair of photon. And so the QKD protocol based on high dimensional hyperentangled state gives rise to a larger coding density and greater security against eavesdropping attacks.

## 4 Conclusions

In conclusion, we have demonstrated a novel scheme for the preparation of a two-photon high dimensional hyperentangled state. Our scheme can encode the state of the two photons into two-dimensional, four-dimensional and four-dimensional entanglement in polarization, frequency and spatial mode respectively by dint of linear optical instruments and cross-Kerr nonlinearity. Theoretically, this scheme is simply extended to higher dimensional qudits and more photons. Furthermore, we have presented a quantum key distribution protocol utilizing the high dimensional hyperentangled state. This protocol is based on the hyperentanglement swapping between frequency and spatial mode. Compared to the normal high dimensional entangled state, the protocol has a higher utilization rate of photon pairs. Meanwhile, the message in our protocol is encoded via a multilevel system which enable us obtain a larger flux of information in comparison with the usual two-dimensional QKD protocols.

### Acknowledgments

This work was supported in part by the National Natural Science Foundation of China(NSFC) under the grants 10935012, 10821063 and 11175249.

## References

- [1] Raussendorf, R.; Briegel, H. J., *Phys. Rev. Lett.* **2001**, 86, 5188-5191.
- [2] Bennett, C.H.; Brassard, C.; Crépeau, C.; Jozsa, R.; Peres, A.; Wootters, W.K., *Phys. Rev. Lett.* **1993**, 70, 1895-1899.
- [3] Wang, C.; Deng, F.G.; Li, Y.S.; Liu, X.S. and Long, G.L., *Phys. Rev. A* **2005**, 71, 044305.
- [4] Bennett, C.H.; Brassard, G.; Popescu, S.; Schumacher, B.; Smolin, J.A.; Wootters, W.K., *Phys. Rev. Lett.* **1996**, 76, 722-725.
- [5] Bruss, D.; Macchiavello, C., *Phys. Rev. Lett.* **2002**, 88, 127901.
- [6] Vaziri, A.; Weihs, G.; Zeilinger, A., *Phys. Rev. Lett.* **2002**, 89, 240401.
- [7] Terriza, G.M.; Vaziri, A.; Řeháček, J.; Hradil, Z.; Zeilinger, A., *Phys. Rev. Lett.* **2004**, 92, 167903.
- [8] Neves, L.; Lima, G.; Aguirre Gómez, J.G.; Monken, C.H.; Saavedra, C.; Pádua, S., *Phys. Rev. Lett.* **2005**, 94, 100501.
- [9] Torres, J.P.; Deyanova, A.; Torner, L., *Phys. Rev. A* **2003**, 67, 052313.
- [10] O'Sullivan-Hale, M.N.; Khan, I.A.; Boyd, R.W.; Howell, J.C., *Phys. Rev. Lett.* **2005**, 94, 220501.
- [11] Kaszlikowski, D.; Gnaniński, P.; Żukowski, M.; Miklaszewski, W.; Zeilinger, A., *Phys. Rev. Lett.* **2000**, 85, 4418.
- [12] Collins, D.; Gisin, N.; Linden, N.; Massar, S.; Popescu, S., *Phys. Rev. Lett.* **2002**, 88, 040404.
- [13] Pasquinucci, H.B.; Peres, A., *Phys. Rev. Lett.* **2000**, 85, 3313.
- [14] Durt, T.; Cerf, N.J.; Gisin, N.; Żukowski, M., *Phys. Rev. A* **2003**, 67, 012311.

- [15] Bourennane, M.; Karlsson, A.; Björk, G., *Phys. Rev. A* **2001**, 64, 012306.
- [16] Cerf, N.J.; Bourennane, M.; Karlsson, A.; Gisin, N., *Phys. Rev. Lett.* **2002**, 88, 127902.
- [17] Du, k.; Qiao, C.F., *J. Mod. Opt.* **2012**, 59, 611-617.
- [18] Rakher, M.T.; Ma, L.J.; Slattery, O.; Tang, X.; Srinivasan, K., *Nature Photonics* **2010**, 4, 786-791.
- [19] Kwiat, P.G.; Mattle, K.; Weinfurter, H.; Zeilinger, A., *Phys. Rev. Lett.* **1995**, 75, 4337-4341.
- [20] Walborn, S.P.; De-Oliveira, A.N.; Thebaldi, R.S.; Monken, C.H., *Phys. Rev. A* **2004**, 69, 023811.
- [21] Simon, C.; Pan, J.W., *Phys. Rev. Lett.* **2002**, 89, 257901.
- [22] Kim, Y.H.; Kulik, S.P.; Chekhova, M.V.; Grice, W.P.; Shih, Y., *Phys. Rev. A* **2003**, 67, 010301.
- [23] Sheng, Y.B.; Deng, F.G.; Zhou, H.Y., *Phys. Rev. A* **2008**, 77, 042308.
- [24] Sheng, Y.B.; Deng, F.G.; Long, G.L., *Phys. Rev. A* **2010**, 82, 032318.
- [25] Nemoto, K.; Munro, W.J., *Phys. Rev. Lett.* **2004**, 93, 250502.
- [26] He, B.; Ren, Y.H.; Bergou, J.A., *Phys. Rev. A* **2009**, 79, 052323.
- [27] Sheng, Y.B.; Deng, F.G., *Phys. Rev. A* **2010**, 81, 032307.
- [28] Vallone, G.; Pomarico, E.; Mataloni, P.; De-Martini, F.; Berardi, V., *Phys. Rev. Lett.* **2007**, 98, 180502.
- [29] Feng, F.Y.; Zhang, Q., *Acta. Phys. Sin.* **2007**, 56, 1924-1927.

## Appendix: Measurement method for 4-dimensional frequency-spatial mode entangled state

Taking photon A for example, we can obtain a one-to-one relationship between the 16 states and the results of measurement by the setup shown in Figure 4 and 5. For the convenience of paper, the 16 states are divided into the following four groups:

$$G_1 : \{|\psi_{11}\rangle_A, |\psi_{12}\rangle_A, |\psi_{13}\rangle_A, |\psi_{14}\rangle_A\}, G_2 : \{|\psi_{21}\rangle_A, |\psi_{22}\rangle_A, |\psi_{23}\rangle_A, |\psi_{24}\rangle_A\},$$

$$G_3 : \{|\psi_{31}\rangle_A, |\psi_{32}\rangle_A, |\psi_{33}\rangle_A, |\psi_{34}\rangle_A\}, G_4 : \{|\psi_{41}\rangle_A, |\psi_{42}\rangle_A, |\psi_{43}\rangle_A, |\psi_{44}\rangle_A\}. \quad (8)$$

We can make use of bit-flip operations to implement the conversions between the states in the same order of different groups, and phase-flip operations to implement the conversions between the states of the same group.

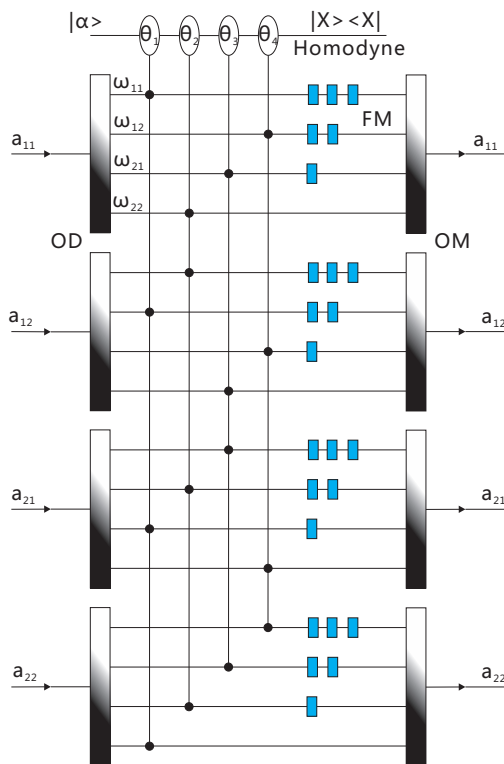


Figure 4: The first part of measurement setup for 4-dimensional frequency-spatial mode entangled state.

In the first part (shown in Figure 4), split every path into four new different paths according to photon's frequency with four optical demultiplexers (OD). Then lead the 16

paths to a cross-kerr nonlinear medium, after measuring the phase shift of the coherent state, we would know which incident state belongs to which group. Concretely, the phase shifts  $\theta_1, \theta_2, \theta_3$  and  $\theta_4$  correspond to  $G_1, G_2, G_3, G_4$  respectively. Afterwards use single-photon frequency multipliers to make the frequencies of all paths the same, that is the information of frequency is erased. Finally, combine the 16 paths into four paths again with four optical multiplexers(OM) [27]. After the first part, the states of spatial mode corresponding to each group are in the following form:

$$\begin{aligned} \varphi_1 &= \frac{1}{2}(|a_{11}\rangle + |a_{12}\rangle + |a_{21}\rangle + |a_{22}\rangle), \varphi_2 = \frac{1}{2}(|a_{11}\rangle - |a_{12}\rangle - |a_{21}\rangle + |a_{22}\rangle), \\ \varphi_3 &= \frac{1}{2}(|a_{11}\rangle - |a_{12}\rangle + |a_{21}\rangle - |a_{22}\rangle), \varphi_4 = \frac{1}{2}(|a_{11}\rangle + |a_{12}\rangle - |a_{21}\rangle - |a_{22}\rangle). \end{aligned} \quad (9)$$

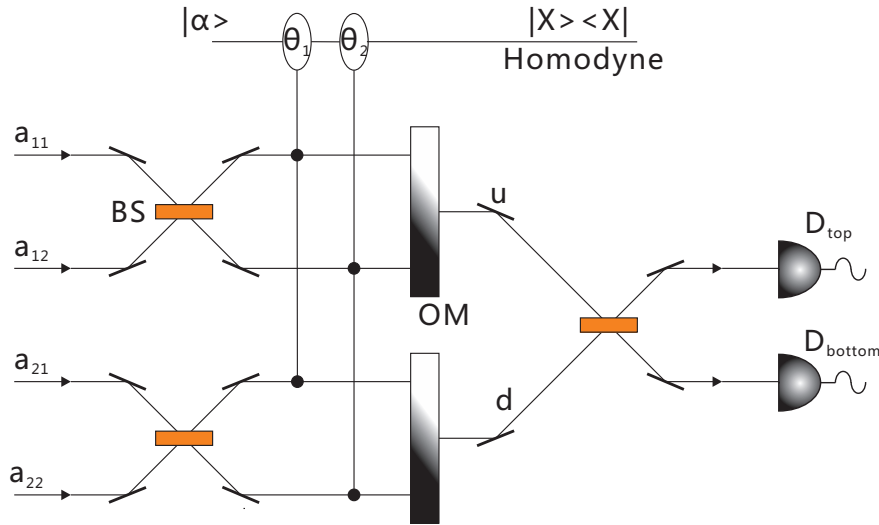


Figure 5: The second part of measurement setup for 4-dimensional frequency-spatial mode entangled state.

In the second part (shown in Figure 5), all the three BSs implement the following transform:

$$\frac{1}{\sqrt{2}}(|T\rangle + |B\rangle) \rightarrow |T\rangle; \frac{1}{\sqrt{2}}(|T\rangle - |B\rangle) \rightarrow |B\rangle. \quad (10)$$

In the same manner, after two BSs, let the paths pass through a cross-kerr nonlinear medium. If the phase shift of coherent state is  $\theta_1$ , that means the input state is  $\varphi_1$  or  $\varphi_4$ , and if the phase shift is  $\theta_2$ , the input state should be  $\varphi_2$  or  $\varphi_3$ . Then combine the upper (under) two

paths into path u (d), and let the paths u and d transit a BS again. As a result, the response of upper (lower) detector indicates the input state is  $\varphi_1$  or  $\varphi_3$  ( $\varphi_2$  or  $\varphi_4$ ).

To sum up, Alice (Bob) can distinguish all the 16 frequency-spatial mode entangled states via our measurement setup.